NASA TECHNICAL NOTE
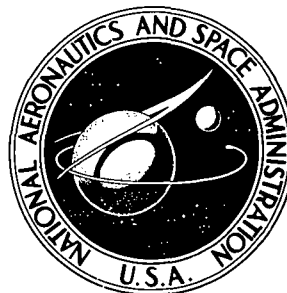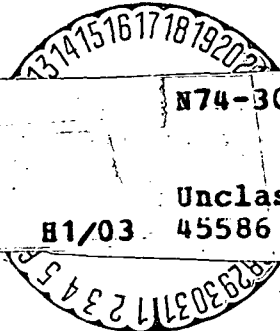
NASA TN D-7757

NASA TN D-7757

TRANSPORT DYNAMICS OF A HIGH-POWER-DENSITY MATRIX-TYPE HYDROGEN-OXYGEN FUEL CELL

by Paul R. Prokopius and Norman H. Hagedorn

Lewis Research Center
Cleveland, Ohio 44135

NATIONAL AERONAUTICS AND SPACE ADMINISTRATION • WASHINGTON, D. C. • AUGUST 1974

1. Report No. NASA TN D-7757	2. Government Accession No.	3. Recipient's Catalog No.
4. Title and Subtitle TRANSPORT DYNAMICS OF A HIGH-POWER-DENSITY MATRIX-TYPE HYDROGEN-OXYGEN FUEL CELL		5. Report Date August 1974
		6. Performing Organization Code
7. Author(s) Paul R. Prokopius and Norman H. Hagedorn		8. Performing Organization Report No. E-7876
9. Performing Organization Name and Address Lewis Research Center National Aeronautics and Space Administration Cleveland, Ohio 44135		10. Work Unit No. 502-25
		11. Contract or Grant No.
12. Sponsoring Agency Name and Address National Aeronautics and Space Administration Washington, D.C. 20546		13. Type of Report and Period Covered Technical Note
		14. Sponsoring Agency Code

15. Supplementary Notes

16. Abstract

Experimental transport dynamics tests have been made on a space power fuel cell of current design. Various operating transients were introduced and transport-related response data were recorded with fluidic humidity sensing instruments. Also, sampled data techniques were developed for measuring the cathode-side electrolyte concentration during transient operation.

17. Key Words (Suggested by Author(s)) Space-power Fuel cell Transport dynamics	18. Distribution Statement Unclassified - unlimited Category 03		
19. Security Classif. (of this report) Unclassified	20. Security Classif. (of this page) Unclassified	21. No. of Pages 19	22. Price* $3.00

TRANSPORT DYNAMICS OF A HIGH-POWER-DENSITY MATRIX-TYPE

HYDROGEN-OXYGEN FUEL CELL

by Paul R. Prokopius and Norman H. Hagedorn

Lewis Research Center

SUMMARY

Experimental transport dynamics tests have been run on a space power fuel cell of current design. The cell tested is a circulating reactant-type matrix cell which has as part of its structure a porous nickel electrolyte reservoir. Various operating transients were introduced and transport-related response data were recorded at both the hydrogen and oxygen sides of the cell with fluidic humidity sensing instruments.

A previously developed mass transport model predicted that the electrolyte contained in the cathode would undergo a drying transient in the time immediately following a load increase. Sampled-data techniques were developed for measuring the cathode side electrolyte concentration during transient operation. Transient concentration data were obtained which bears out the prediction of cathode-side concentration changes. However, at the conditions tested, it was found that the severity or magnitude of any transient would not be detrimental to cell operation.

The water transport data taken at the anode illustrate the transient rate of product water outflow from the cell. The cell with an electrolyte reservoir, compared to one having no reservoir, was found to have a much smaller net water loss when subjected to a step increase in load.

INTRODUCTION

In H_2-O_2 fuel cells the product of the electrochemical reaction is water. The removal of this product water at a rate which regulates the water inventory of the cell electrolyte within its design limits is a prime requisite for proper cell operation. The design of systems needed to achieve this type of control could be greatly aided by gaining an understanding of the mechanisms that regulate the movement and hence the rejection of product water from an operating cell. Therefore an on-going program is being con-

ducted at the Lewis Research Center to study fuel cell transport processes on both an experimental and analytical basis (refs. 1 to 3). Thus far in the analytical portion of the program, a mathematical mass transport model has been developed to simulate the processes controlling fuel cell water transport, for both steady-state and transient operation, when the product water is rejected to a flowing stream of hydrogen. In the experimental portion, a fluidic humidity sensor was developed as a readout device for obtaining transport-related experimental data (ref. 4). The sensor provides a continuous reading of the humidity of the effluent reactant and this, in turn, can be used to determine the outflow of water from the cell. With the sensor as part of a fuel cell dynamics test apparatus (ref. 3), transport dynamics studies have been run on both molten alkaline-electrolyte cells (Bacon cells) and on low temperature alkaline matrix cells. In these cells all the electrolyte was contained between and within the electrode structures. Between the electrodes, the electrolyte existed either as a free liquid (Bacon cell) or was constrained within an asbestos matrix (low temperature alkaline-electrolyte cells).

The study being reported on here was also conducted on a matrix-type cell. However, this cell has as part of its structure a porous nickel electrolyte reservoir which is located between the hydrogen supply chamber and the anode (fig. 1(a)). The purpose of this reservoir is to contain a large portion of the cell's electrolyte in a volume outside of the electrode-matrix structure. This minimizes the effects that electrolyte volume excursions have on cell performance.

A qualitative application of our mathematical mass transport model to this cell predicted that cathode electrolyte drying transients would occur in the time immediately following a load current increase. To determine whether these drying transients do in fact occur, and to what extent, sampled-data oxygen-side humidity measuring techniques were developed. These techniques provide a method for observing the concentration transients resulting from step disturbances in cell load and operating conditions. Also, continuous hydrogen stream humidity data were taken to elucidate the overall water rejection response of this particular cell.

APPARATUS AND INSTRUMENTATION

Fuel Cell

A schematic diagram and a cutaway view of the type of matrix cell tested are shown in figure 1. The cell assembly consists of an anode, cathode, matrix, electrolyte reservoir plate, and a unitizing support frame. The cell active electrode area is 0.0464 square meter (72 in.^{2}). The anode and cathode are constructed of a fine mesh

silver-plated nickel screen which is catalyzed with a platinum/palladium and teflon mixture. Both electrodes are 0.014 centimeter (5.5 mils) thick. The electrolyte reservoir plate is a 0.254-centimeter- (100-mil-) thick porous nickel sinter and the matrix is a 0.0254-centimeter- (10-mil-) thick sheet of fuel-cell grade asbestos. The cell electrolyte is aqueous potassium hydroxide at a concentration of approximately 30 percent potassium hydroxide by weight. Waste heat is removed from the cell by flowing a liquid coolant through a chamber which covers the back of the hydrogen reactant chamber. The coolant system is used to control the cell temperature between 361 and 394 K (190° and 250° F).

Product water is removed from the cell by flowing an excess of humidity-controlled hydrogen through the hydrogen supply chamber. In a steady-state mode of operation the product water diffuses from the reaction sites within the anode structure into the electrolyte reservoir. It is evaporated from the electrolyte contained by the reservoir into the hydrogen supply chamber from whence it is removed from the cell by the reactant stream.

Oxygen flows on demand into the normally dead-ended oxygen supply chamber.

Test Apparatus

The fuel cell dynamics test apparatus was used to generate the mixture of hydrogen and water vapor on which the fuel cell was operated. The rig (detailed description given in ref. 3) is composed of closed-loop controllers which are capable of controlling with a high degree of accuracy the reactant stream parameters of temperature, pressure, flow rate, and humidity. Aside from being able to provide an accurately controlled steady flow, the test apparatus has the dynamics testing capability to produce fast perturbations in any one of the stream parameters while automatically holding the other parameters constant. This individual control characteristic eliminates parameter confounding and thus provides the capability to isolate individual parameter effects on cell performance.

Humidity (Concentration) Sensing Instruments

In fuel cell applications, data from the fluidic humidity (mass ratio) sensor can be utilized in either of two ways. It can be used to determine the actual water outflow from a circulating reactant-type cell and hence determine the transient and net changes in cell electrolyte water content, or it can be used to determine the electrolyte concentration in the area of the reactant outlet port for an intermittently flowing reactant.

To find the water outflow for an operating fuel cell, the fluidic sensor is used to obtain a continuous reading of the mass ratio (humidity) of the effluent reactant stream.

3

When this is combined with the known composition of the reactant supplied the cell, the stoichiometric reactant consumption rate and the water formation rate (both of which are proportional to cell current), a continuous calculation of the rate at which water is rejected from the cell is attainable. The water rejection data can, in turn, provide a measure of the all-important dependent variable, the electrolyte volume.

In determining the electrolyte concentration, the effluent stream mass ratio is again the recorded parameter. If the stream in question is assumed to be a mixture of ideal gases, the component mole ratio defines the ratio of the component partial pressures as

$$\frac{\Gamma_1}{\Gamma_2} = \frac{P_1}{P_2}$$

or

$$\frac{W_1}{W_2} = \left(\frac{P_1}{P_T - P_1}\right)\frac{M_1}{M_2}$$

In these expressions the terms Γ_1 and Γ_2 represent the numbers of moles of each component, P_1 and P_2 the respective partial pressures, W_1 and W_2 the mass flow rates, P_T the ambient mixture pressure, and M_1 and M_2 the component molecular weights. The mass ratio W_1/W_2, therefore, can be used to obtain the partial pressure of either stream component. Installed in an intermittently flowing reactant stream, the mass ratio sensor is used to determine the stream vapor pressure. For the types of cells tested, the typical and apparently valid assumption is that the reactant stream equilibrates with the cell electrolyte by the time it reaches the reactant exit port. That is, the vapor pressure of the electrolyte in the area of the outlet port and the partial pressure of the water vapor in the reactant stream flowing over that region are equal. The fluidic sensor reading can thereby be used to determine the electrolyte vapor pressure at the outlet port which, when applied to experimentally obtained vapor pressure-concentration relations, provides a reading of cell electrolyte concentration in this area.

The cell tested was instrumented with mass flow ratio (humidity) sensing devices at both the anode and cathode. The main element of each sensor is a fluidic, delay-line oscillator. Schematics of the oscillator and the complete H_2-humidity sensor are shown in figure 2. The oscillator is designed so that the stream flowing through the nozzle attaches itself to one of the two stream attachment walls and remains fixed there until a pressure pulse produced by the stream traverses the delay line of the side to which it is attached. This pulse forces the stream to the opposite attachment wall, whereupon the process is repeated and an oscillation established. The frequency of the oscillation is a

4

function of the delay line pulse propagation time, and is measured by porting one of the delay lines to a dynamic transducer to pick up the pressure pulsations setup by the oscillating stream. The frequency of these pulsations is a function of the molecular weight of the stream in question at a given temperature and pressure. Since the stream molecular weight is a function of its mass ratio, a calibration curve of oscillation frequency as a function of mass ratio (humidity) can be obtained. To obtain a readable humidity signal from the instrument (fig. 2) the pulsating charge output of the fluidic oscillator is fed to a charge amplifier to be converted to a periodic voltage and from there to a frequency-to-dc converter which provides a recordable humidity analog. A more detailed description of the humidity sensor is given in reference 4.

As shown in figure 2, a sensor was installed in the hydrogen stream at the anode reactant chamber outlet to provide a continuous reading of the outlet hydrogen stream mass ratio and hence the rate at which water is rejected from the cell. The oxygen stream of the cell tested is normally dead-ended and thus does not provide a continuous-flowing reactant to drive a fluidic sensor. To obtain a cathode-electrolyte concentration reading, a sampled-data sensing technique was devised. A schematic of this system is shown in figure 3. In this system the O_2-H_2O gas mixture is sampled by periodically opening a solenoid valve installed in the exit line of the fluidic oscillator. The solenoid is driven by an electronic timer which is set up with the sampling pulse shown in the insert. The solenoid is open and gas flows for 8 seconds of the total 32-second pulse cycle. The oscillator that was used in the system was designed with an extremely small inlet nozzle (0.0127 by 0.0254 cm (0.005 by 0.010 in.)) and thus a minimal amount of gas flow was required to establish an oscillation. The rate of water withdrawal from the cell by the sample stream is less than 2 percent of the 18.6-ampere-per-square-meter (200-A/ft^2) rate of water consumption at the cathode. At this net flow, in 1 hour of continuous sampling, the amount of water removed from the cell by the sample stream would amount to about 1 percent of the water contained in the cell's electrolyte. Therefore, the sampling of the cathode gas mixture has a negligible effect on the cells overall water balance. To determine whether the sampling technique affected the electrolyte concentration near the O_2 exit port, the following check was made: two sets of four data pulses each were taken, with a 20-minute interval separating the sets. After another 20-minute interval of no data, continuous sampling was maintained for an hour. The humidity of the O_2 stream did not vary during the 1 hour of continuous sampling, and was identical to that measured during the discrete sample sets. It was, therefore, concluded that the sampling technique had no significant effect on the collected data.

The signal conditioner of the sampled data system consists of several components, two of which are a charge amplifier and a frequency-to-dc converter. The output of the oscillator's dynamic transducer is a high impedance charge signal unsuitable as an input to any readout device. Therefore, the transducer's output is fed to a charge amplifier

to be converted to a low impedance periodic voltage. This can then serve as an input to a frequency-to-dc converter to obtain a dc analog readout of the oscillator frequency. From the converter the analog signal is fed to a "dead time" generator which blocks the signal for the first 2 seconds of the 8-second flow pulse. This allows time for the gas trapped in the oscillator from the previous data pulse to be purged from the system. Actual data is then taken on a fresh sample from the last 6 seconds of the flow pulse. This signal is integrated over the 6-second period to average out some of the electronic noise and it is finally recorded on a strip chart recorder.

Sample recordings from both humidity sensors are shown in figure 4. These data were taken for a step in load from 20 to 200 amperes and from 200 back to 20 amperes. The hydrogen humidity sensor shows a base-to-peak change in outlet stream water flow from 0.161 to 0.222 kilograms per hour (0.355 to 0.488 pph) and the O_2 humidity sensor displays a base-to-peak change in cathode electrolyte concentration from approximately 34 to 37.5 percent. To improve the resolution of the oxygen sensor data in the time immediately following the transient, the pulse cycle "off time" was shortened from 24 to approximately 12 seconds.

TEST PROCEDURE

With the cells reactant supply chamber purged and then filled with nitrogen, the liquid coolant was circulated through the cell at 361 K (190° F) (inlet) and the oven in which the cell was installed was heated to bring the cell to its operating temperature of 361 K (190° F). Once this temperature was attained, the reactants were introduced and the cell electrolyte concentration was allowed to equilibrate at open circuit to the value desired for a particular test. This concentration was dictated by setting the hydrogen water-vapor partial pressure (humidity) equal to the electrolyte vapor pressure corresponding to the desired concentration. After the load was introduced, a steady-state operating condition was realized when the startup transients in the continuously monitored parameters of cell temperature, voltage, and current were damped out and when the water vapor outflow measured by the hydrogen humidity sensor equaled the water input plus water generated by the cell reaction.

Once steady-state was attained, dynamics tests were conducted by disturbing the rate at which water is produced in the cell. The water production transients were step functions of load current introduced by an electronic load bank. The resulting response transients were recorded with the fluidic sensors as changes in the hydrogen and oxygen stream outlet humidities. For analysis, these data were converted to water rejection rate changes from the anode and electrolyte concentration changes at the cathode, as described previously.

RESULTS AND DISCUSSION

The transient response of the cell outlet water vapor flow rate to a 0- to 100-ampere step in cell load is shown in figure 5. The response reflects the readjustment of the electrolyte concentration to an equilibrium value at which the effective vapor pressure difference between the cell electrolyte and the hydrogen stream is sufficiently large to drive the product water from the cell structure. For approximately the first 3 minutes, the transient shows the cell electrolyte absorbing a net amount of the water produced at the anode. During the remainder of the transient, a net amount of water is rejected from the electrolyte. The shaded area to the left of the transient curve represents the mass of water absorbed by the electrolyte and the shaded area under the overshoot portion of the transient represents the mass of water that was rejected by the electrolyte. The difference between these two areas represents the net amount of water that was rejected/absorbed over the duration of the transient.

The purpose of the electrolyte reservoir in this cell is to add electrolyte volume capacity to the cell structure. Its effect is to absorb the electrolyte volume changes that would otherwise occur within the electrode-matrix assembly as the cell is put through its operating profile. The effect that the reservoir has on the water rejection characteristic of the cell can be seen by comparing the response shown in figure 5 to a comparable transient of a previously tested cell which had no reservoir. To provide a basis for comparison, the response curves for the transients were normalized by plotting each data point as a ratio of the change in the water vapor component of the hydrogen outlet stream to the total change between the initial and final equilibrium values. This comparison is made in figure 6. As one might expect, the cell without the porous reservoir plate displayed a much faster initial rise time and had a very pronounced underdamped (overshoot) characteristic, indicating considerable drying of the electrolyte. Thus, the addition of the reservoir component is seen to have a strong capacitive or damping effect on the water rejection process.

Though data such as that of figure 6 can be used to identify the characteristic of the overall water rejection process, it does little in defining parameters such as the changing electrolyte concentration within the anode. Since the reservoir is an integral part of the cell structure, it is impossible to obtain experimental data to identify anode concentration characteristics. Analytical techniques such as those developed in the mathematical model (ref. 3) would have to be resorted to. However, concentration can be determined on the cathode side by the techniques described previously. Actually, in cells such as the one tested, interest centers on the cathode side of the cell since this is typically where the electrolyte in the electrode-matrix structure is the driest. Also, phenomena such as localized drying in the area of the oxygen inlet port can be of concern if the cell is supplied by a dry O_2 stream.

A cathode-side concentration transient is shown in figure 7. These data show the load step response of the concentration of the electrolyte contained by the cathode in the area of the oxygen outlet port. For this cell the 20- to 200-ampere load step is equivalent to a low to nominal power step for the fuel cell system for which the cell was designed. The transient shows a drying characteristic which is seen to peak approximately 20 seconds after the load disturbance is introduced. For a period of approximately 40 seconds, thereafter, the concentration drops. This drop reverses at about 60 seconds and from then on the concentration begins a slow rise toward the final steady-state value of 39.8 percent. The occurrence of the initial post-transient drying peak was predicted by the mathematical mass transport model (ref. 3). The model indicates that this drying results from the fact that the water required by the cathode reaction cannot be supplied instantaneously. In a normal steady-state mode the water consumed by the cathode is transported by diffusion from the anode where it is generated. Upon introducing the load transient, the rates of water production and consumption increase instantaneously, however, the diffusive transport introduces a lag in the rate at which water is transported across the cell. During this lag period, the electrolyte which is near the cathode reaction zone supplies some of the water required by the reaction, the result being a drying or concentrating effect on the cathode electrolyte.

In the transient of figure 7, following the initial drying period, the cathode electrolyte has a tendency toward a wetter or less concentrated condition. However, after 60 seconds have elapsed, the cell temperature becomes the dominant factor and the concentration is driven to a drier final value. That is, the heat generated by the cell reaction causes a cell temperature rise. The increasing cell temperature raises the electrolyte vapor pressure and water is driven from the electrolyte into the flowing H_2 stream.

Since the cathode concentration data were obtained from a humidity sensor which, in effect, measures electrolyte vapor pressure, a temperature correction was required in converting the raw sampled data into the form shown in figure 7. An example of a thermal transient generated by a load step (20 to 200 A) is shown in figure 8. These data were taken with a quick-response thermocouple probe that was installed in the oxygen chamber immediately above the electrolyte whose concentration was being measured.

Assuming the measured electrolyte concentration at the cathode outlet can be used as an indication of the overall cathode electrolyte concentration, one characteristic of this cell seems to be its tendency to go to a less concentrated (wetter) condition after the cell load is increased. This is shown in the transient of figure 7 as a drop in concentration following the initial drying peak. One would assume that as the load is increased more water is required by the cathode reaction, thus requiring a steeper concentration gradient from anode-to-cathode and hence a drier cathode electrolyte in the final steady-state mode. However, the presence of the electrolyte reservoir in this cell apparently

8

causes a distribution of the concentration gradients within the cell such that, were it not for an increase in cell temperature, the cathode electrolyte would end up in a wetter state. This wetting tendency is beneficial in that it tends to attenuate the magnitude of the drying transients. In a matrix cell with no reservoir plate, or a very thin one, an inherent drying tendency would exist. This would add to the transient drying, the result being an increase in the severity of the drying peak.

In running various transients one of the parameters which was seen to affect the magnitude of the short-term drying spike was the initial electrolyte concentration (i.e., the concentration established at open circuit by the hydrogen stream being supplied to the cell). This effect is illustrated in figure 9 in which the magnitude of the drying transient at the cathode exit is plotted against the initial electrolyte concentration. For all the data points, the same 20- to 200-ampere load step was introduced and the coolant inlet was held at a constant 361 K (190° F). Thus, the thermal effects on the concentration were the same for each data point and therefore should have no influence on the characteristic being illustrated. The plot of figure 9 displays a very nonlinear characteristic thus suggesting that the transport processes controlling the concentration are likewise nonlinear.

For the type of cell tested, dry oxygen is normally supplied to a dead-ended reactant chamber. As the dry demand-flow stream passes over the cathode electrolyte, it evaporates water until it saturates with respect to the electrolyte. This electrolyte drying that results is the most severe in the area of the oxygen inlet port. To determine the degree to which this drying occurs, a measurement technique was devised to obtain an approximation of this concentration with the cell in a steady-state operating mode. To obtain this concentration reading the cells oxygen supply plumbing was arranged so that the direction of flow between its inlet and purge ports could be instantaneously reversed. Then with the cell under load and operating in a steady-state mode, and the oxygen sampling system in operation, the oxygen flow direction was reversed and the ensuing transient observed. The transient represents the reequilibration (rewetting) of the electrolyte in the inlet port area that is brought about by shutting off the dry oxygen stream. A typical response is shown in figure 10. With the data pulse period set at 20 seconds, the first data point in the reequilibration transient occurred 20 seconds after the flow direction was reversed. After the transient was traced out, it was back-extrapolated to time zero to provide a reasonable approximation of the steady-state electrolyte concentration at the oxygen inlet port. For the case shown in figure 10 this value is 41.2 percent. At this set of operating conditions this concentration poses no problem.

CONCLUDING REMARKS

The electrolyte reservoir has a strong capacitive or damping effect on the cell's water rejection process. This was shown by comparing the water rejection response transients for the cell tested in this study to comparable transients of a previously tested matrix-type cell which had no reservoir. The rate at which product water is rejected into the hydrogen stream in response to a step in the rate of water production (cell load) was the type of data compared. These data show that the cell without the reservoir displays a much larger underdamped (overshoot) characteristic and a much faster rise time. Also, the data show that the cell with no reservoir suffers a much larger loss of electrolyte-water as the result of the water production (load step) transient.

Prior to starting the dynamics tests the mathematical mass transport model developed in previous work was qualitatively applied to the matrix cell being tested. The model predicted that the cathode electrolyte would undergo a drying transient in the time immediately following the introduction of a load increase. As seen in the experimental data this prediction was borne out. For the cell tested the observed transients did not represent any severe conditions; however, off-design cell operation was not explored.

The cells geometric parameters obviously have a significant effect on its transient response. Of particular importance is the size (thickness) of the electrolyte reservoir. An intuitive deduction suggests that the short-term drying transients would increase in magnitude if the reservoir were made thinner.
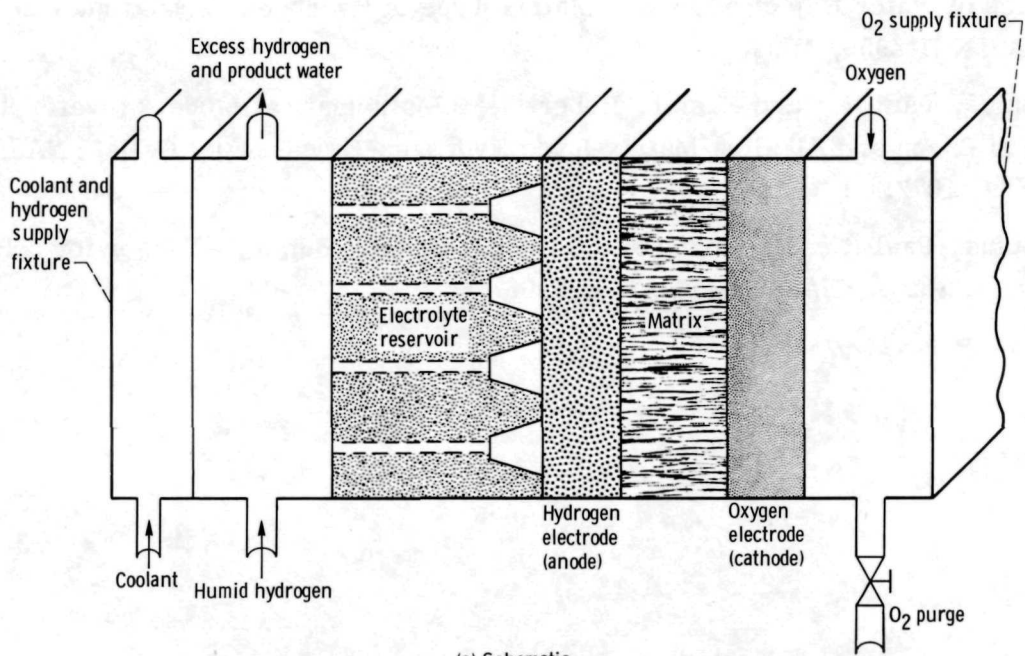
To facilitate making oxygen-side electrolyte concentration measurements, sampled-data techniques have been developed which have, in effect, expanded our transport dynamics testing capability to include cells with dead-ended reactant supplies, such as those embodying static water removal.

Lewis Research Center,
    National Aeronautics and Space Administration,
        Cleveland, Ohio, May 9, 1974,
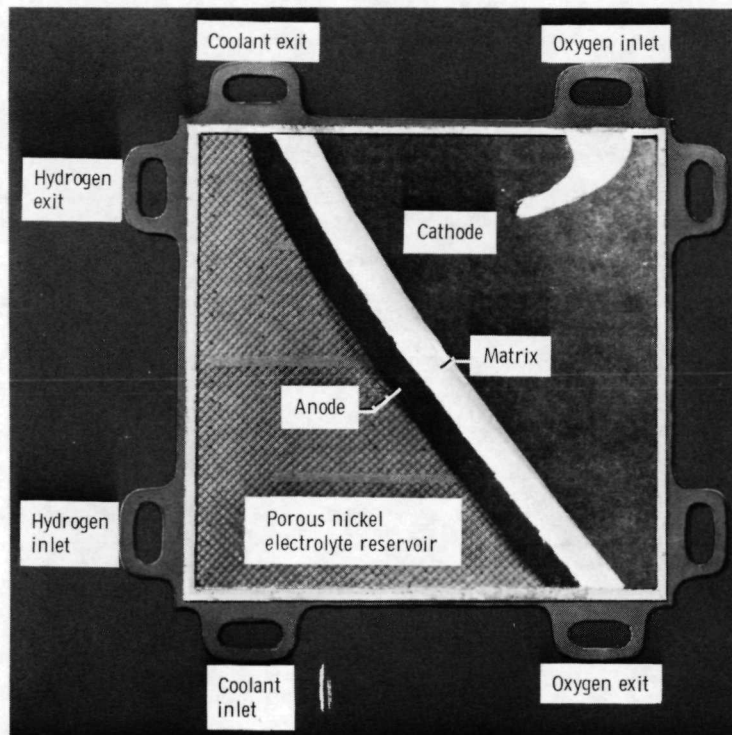   502-25.

REFERENCES

1. Prokopius, Paul R.; and Hagedorn, Norman H.: Investigation of the Dynamics of Water Rejection from a Hydrogen-Oxygen Fuel Cell to a Hydrogen Stream. NASA TN D-4201, 1967.

2. Prokopius, Paul R.; and Easter, Robert W.: Experimental Investigation of the Dynamics of Water Rejection from a Matrix Type of Hydrogen-Oxygen Fuel Cell. NASA TN D-4956, 1968.

3. Prokopius, Paul R.; and Easter, Robert W.: Mathematical Model of Water Transport in Bacon and Alkaline Matrix-Type Hydrogen-Oxygen Fuel Cells. NASA TN D-6609, 1972.

4. Prokopius, Paul R.: Use of a Fluidic Oscillator as a Humidity Sensor for a Hydrogen-Steam Mixture. NASA TM X-1269, 1966.

Excess hydrogen
and product water

O_2 supply fixture

Oxygen

Coolant and
hydrogen
supply
fixture

Electrolyte
reservoir

Matrix

Hydrogen
electrode
(anode)

Oxygen
electrode
(cathode)

Coolant   Humid hydrogen

O_2 purge

(a) Schematic.

Coolant exit   Oxygen inlet

Hydrogen
exit

Cathode

Matrix

Anode

Hydrogen
inlet

Porous nickel
electrolyte reservoir

Coolant
inlet

Oxygen exit

(b) Cutaway.
Figure 1. – Fuel cell.
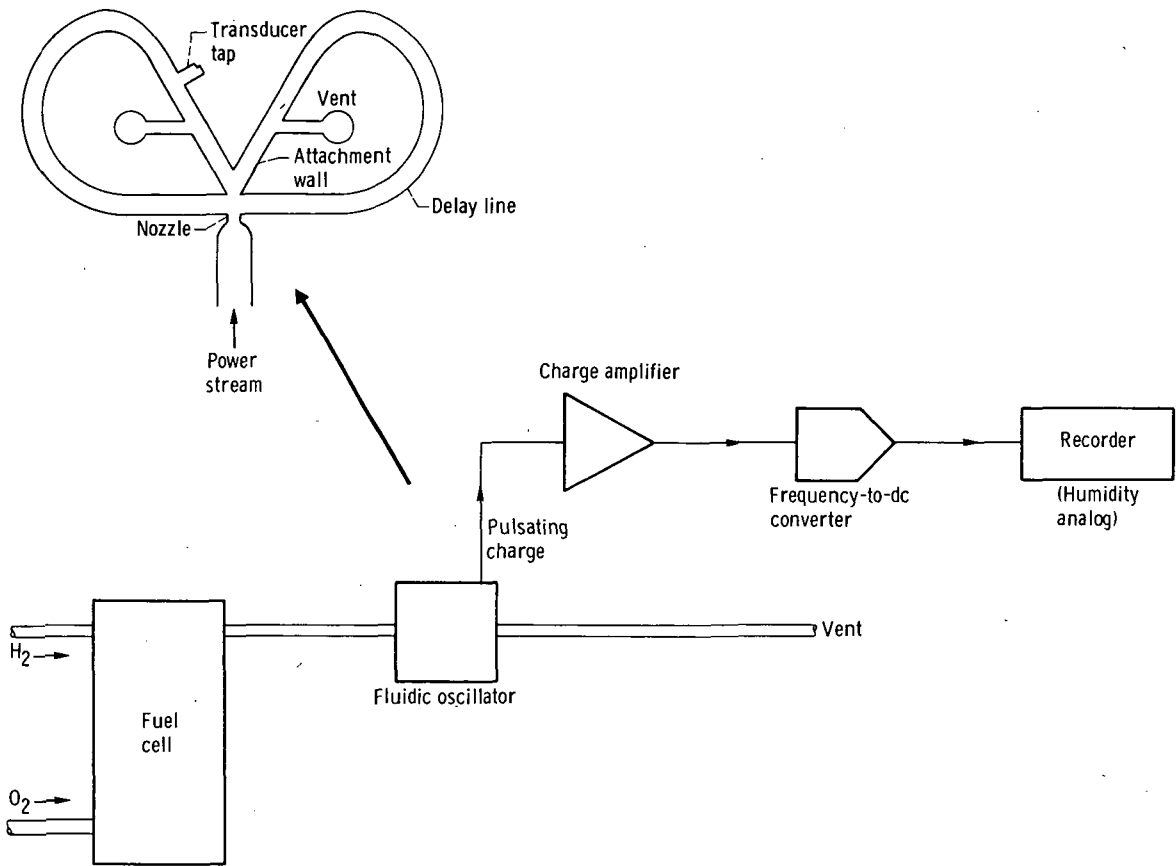
Figure 2. - Schematic of fluidic oscillator and hydrogen humidity sensor. Pure hydrogen oscillation frequency, ~3000 hertz; instrument accuracy, ± 2 percent (electronics limiting).

H_2 humidity sensor
(continuous reading)

O_2

Sampling pulse

On

Off

8 sec   24 sec

Fuel cell
assembly

H_2   O_2

Electronic
timer

Solenoid

O_2 humidity sensor
(sampled data)

Vent

H_2

Signal
conditioner

Integrator

Strip
chart
recorder
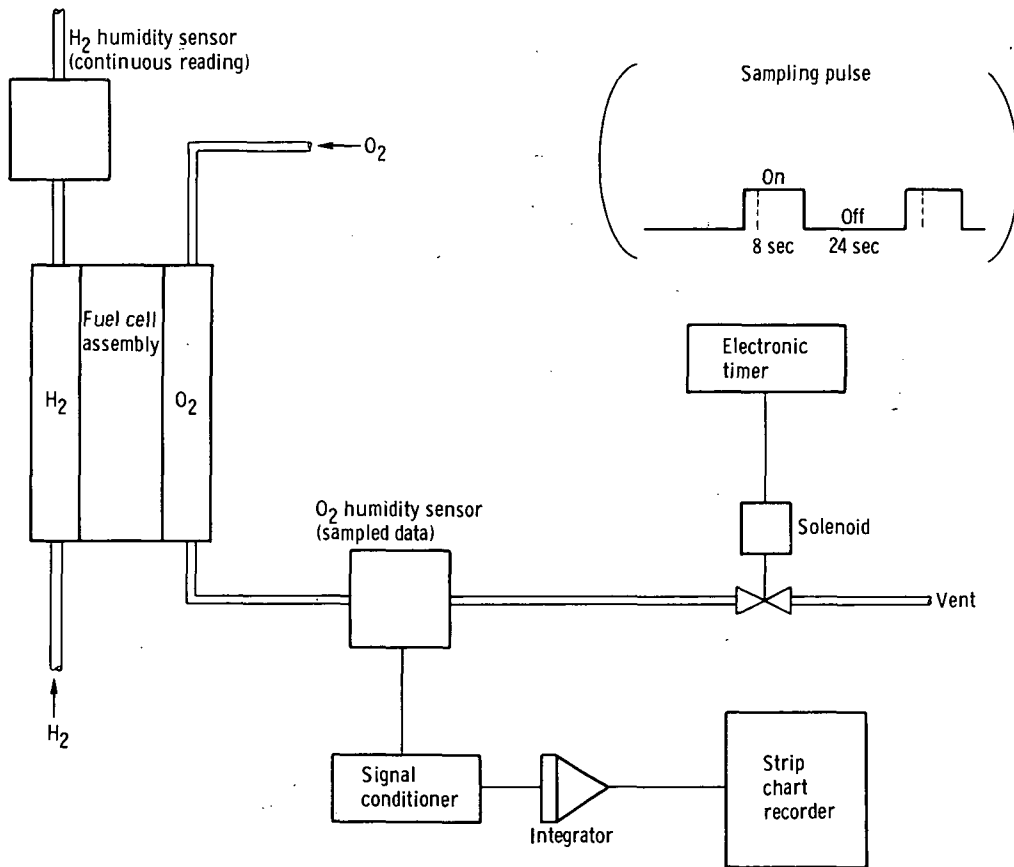
Figure 3. – Schematic of concentration metering.
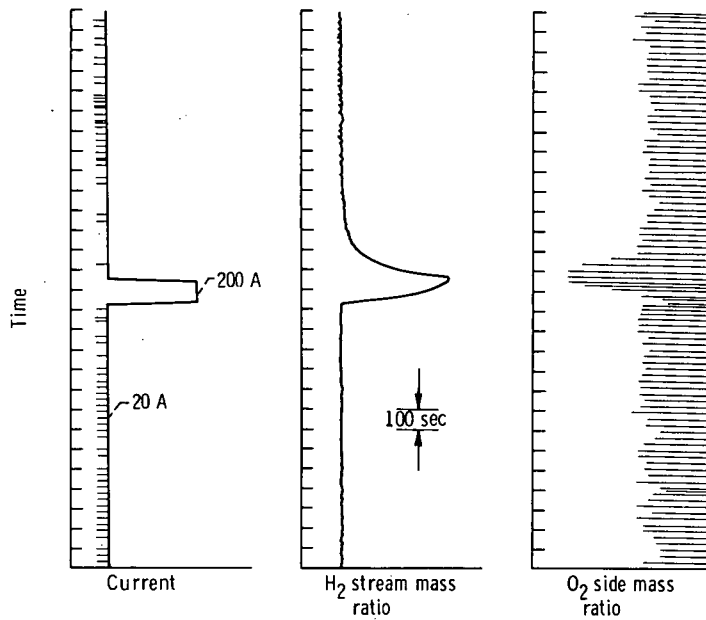
(a) Load current, 20 to 200 amperes.

(b) H_2 humidity sensor.

(c) O_2 humidity sensor.

Figure 4. - Sample humidity sensor recordings for 20- to 200-ampere load step.
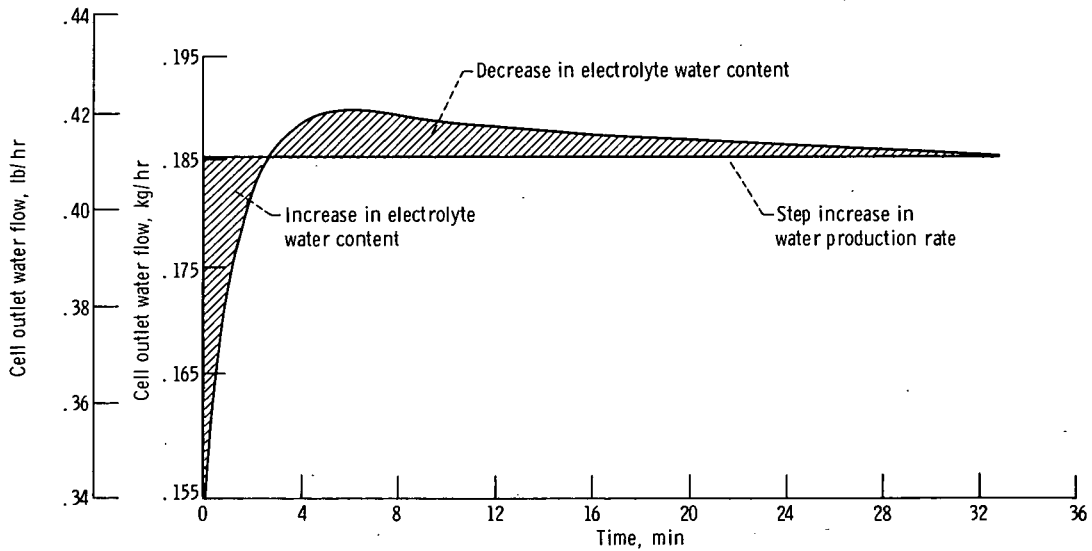
Figure 5. - Transient response of water-vapor-component flow of cell outlet hydrogen stream to step in cell load. Operating conditions: inlet hydrogen-component flow, 0.0544 kilogram per hour (0.12 lb/hr); inlet water-vapor-component flow, 0.154 kilogram per hour (0.34 lb/hr); load step, 0 to 100 amperes.
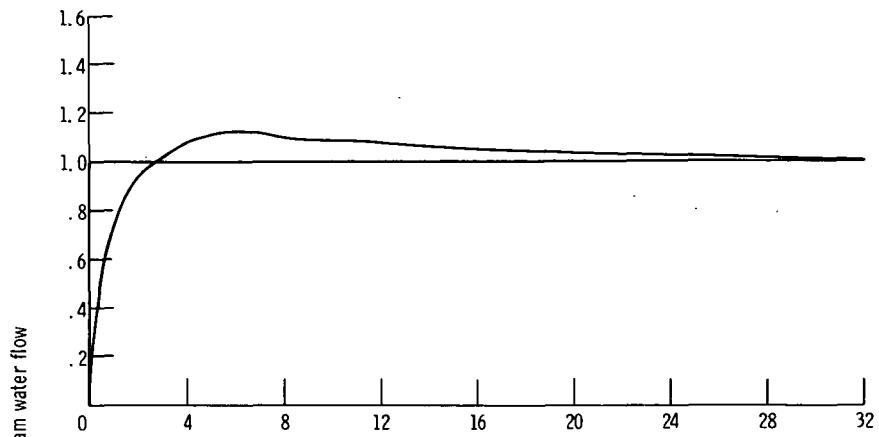
(a) With electrolyte reservoir (data from transient of fig. 5).
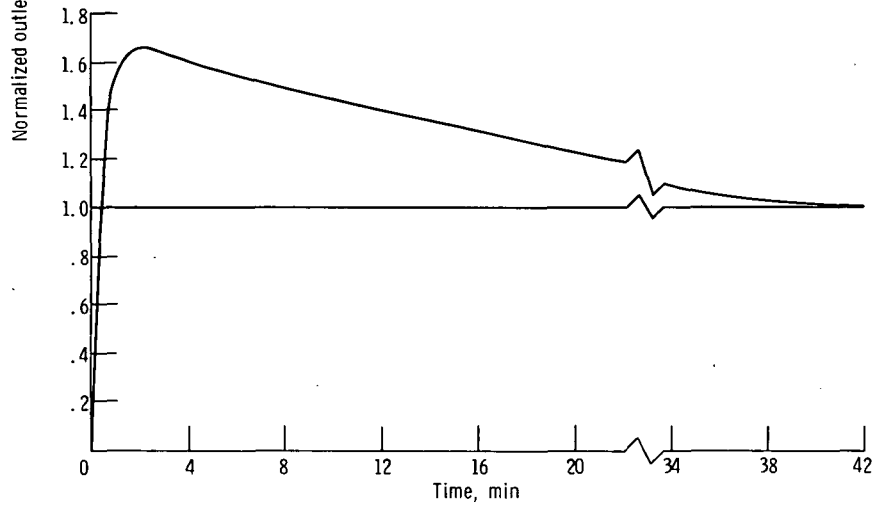
(b) Without electrolyte reservoir (data from fig. 14, ref. 2).

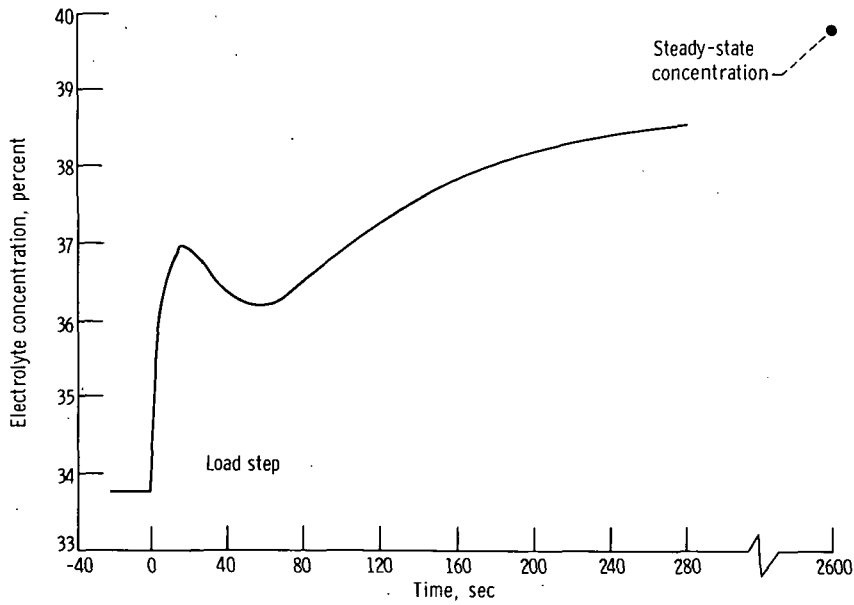Figure 6. – Normalized load step transient response of cell.

Figure 7. - Load step response of cathode electrolyte concentration at oxygen outlet port. Load step, 20 to 200 amperes; hydrogen inlet stream 32 percent KOH; coolant inlet temperature, 361 K (190° F).
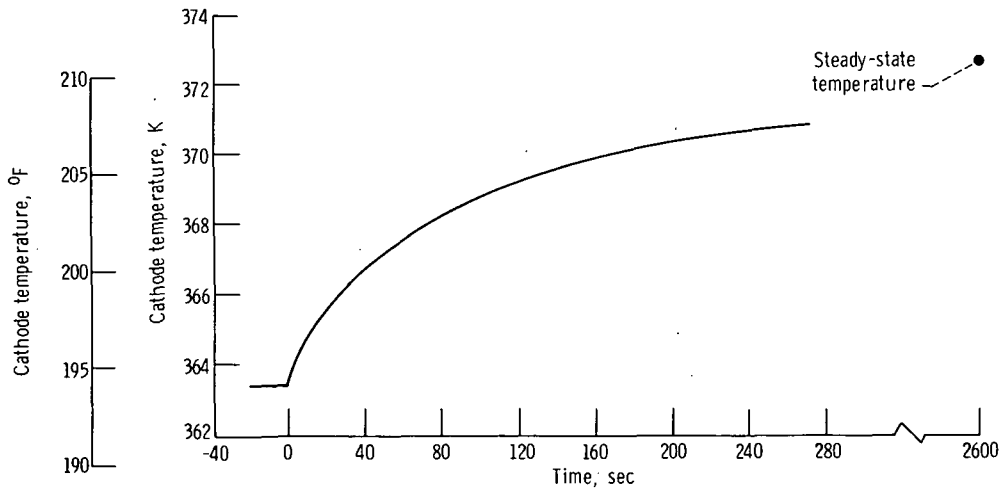

Figure 8. - Temperature response of cathode at oxygen outlet port for 20- to 200-ampere load step.
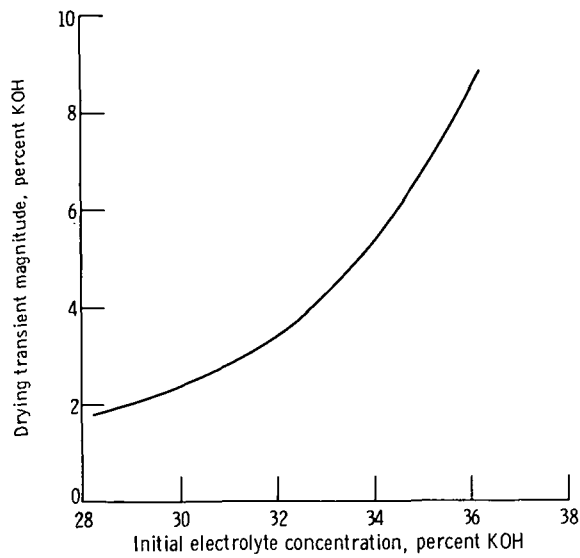
Figure 9. - Hydrogen stream humidity effect on drying spike magnitude. Load step, 20 to 200 amperes; coolant inlet temperature, 361 K (190° F).
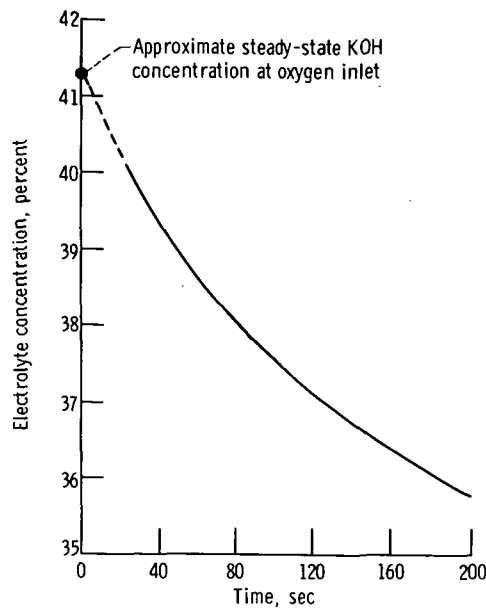

Figure 10. - Response of cathode electrolyte concentration at oxygen inlet port for reversal in oxygen flow direction.

"The aeronautical and space activities of the United States shall be conducted so as to contribute . . . to the expansion of human knowledge of phenomena in the atmosphere and space. The Administration shall provide for the widest practicable and appropriate dissemination of information concerning its activities and the results thereof."

—NATIONAL AERONAUTICS AND SPACE ACT OF 1958

NASA SCIENTIFIC AND TECHNICAL PUBLICATIONS

TECHNICAL REPORTS: Scientific and technical information considered important, complete, and a lasting contribution to existing knowledge.

TECHNICAL NOTES: Information less broad in scope but nevertheless of importance as a contribution to existing knowledge.

TECHNICAL MEMORANDUMS: Information receiving limited distribution because of preliminary data, security classification, or other reasons. Also includes conference proceedings with either limited or unlimited distribution.

CONTRACTOR REPORTS: Scientific and technical information generated under a NASA contract or grant and considered an important contribution to existing knowledge.

TECHNICAL TRANSLATIONS: Information published in a foreign language considered to merit NASA distribution in English.

SPECIAL PUBLICATIONS: Information derived from or of value to NASA activities. Publications include final reports of major projects, monographs, data compilations, handbooks, sourcebooks, and special bibliographies.

TECHNOLOGY UTILIZATION PUBLICATIONS: Information on technology used by NASA that may be of particular interest in commercial and other non-aerospace applications. Publications include Tech Briefs, Technology Utilization Reports and Technology Surveys.

Details on the availability of these publications may be obtained from:

SCIENTIFIC AND TECHNICAL INFORMATION OFFICE

NATIONAL AERONAUTICS AND SPACE ADMINISTRATION
Washington, D.C. 20546